Advances in Ophthalmology Practice and Research 3 (2023) 119–125

Contents lists available at ScienceDirect

Advances in Ophthalmology Practice and Research

journal homepage: www.journals.elsevier.com/advances-in-ophthalmology-practice-and-research

Full Length Article

Quantification of vascular morphology in optical coherence tomography angiography in primary open angle glaucoma

Praneeth Kalva [a,*], Rubeel Akram [a], Priya Mekala [a], Monica Patel [a], Sruthi Suresh [a], Karanjit S. Kooner [a,b]

[a] Department of Ophthalmology, University of Texas at Southwestern Medical Center, Dallas, TX, USA
[b] Department of Ophthalmology, Veteran Affairs North Texas Health Care Medical Center, Dallas, TX, USA

ARTICLE INFO

Keywords:
Optical coherence tomography angiography
Glaucoma
Vessel density

ABSTRACT

Purpose: To quantitatively measure and compare the vascular morphology in healthy eyes and eyes with primary open-angle glaucoma (POAG) using optical coherence tomography angiography (OCTA) scans.
Methods: This is a retrospective and cross-sectional study which include healthy individuals and individuals with POAG that underwent OCTA imaging at an academic center's glaucoma clinic. We analyzed OCTA scans of the macula and optic nerve head (ONH) of one eye from each subject to quantitatively measure vessel density (VD), vessel length density (VLD), and branchpoint density (BPD). We compared these 3 parameters between the healthy and POAG groups and used logistic regression classification models to determine their diagnostic value in differentiating healthy and glaucomatous eyes.
Results: We included 49 healthy subjects and 49 subjects with POAG. After age-adjusted analysis, the parameters of VD, VLD, and BPD were significantly reduced in eyes with POAG ($P < 0.001$) in all scan layers and most significantly around the ONH. The parameter with the best performances were radial peripapillary capillary (RPC) VD [AUC (areas under the curve): 0.939 (0.891, 0.987)] which had statistically higher performances ($P < 0.05$) than parameters in the superficial or deep layers. All 3 parameters in the RPC layer had statistically similar performances.
Conclusions: We found that VD, VLD, and BPD were reduced in glaucomatous eyes. The morphologic parameters of VLD and BPD had similar performances to the traditional parameter of VD in RPC layers. Our results suggest that vascular morphology parameters may provide additional value in the diagnosis and evaluation of glaucoma.

1. Introduction

Glaucoma is a vision-threatening optic neuropathy characterized by progressive degeneration of retinal ganglion cells.[1] Vascular health has been theorized to play an important role in the progression of glaucoma. Reduction in ocular blood supply is hypothesized to be a cause of retinal ganglion cell death, resulting in glaucoma with or without changes in intraocular pressure (IOP).[2] Although it remains unclear whether vascular damage precedes retinal ganglion cell damage or vice versa, information about the underlying vasculature of the eye may be helpful for clinicians in the diagnosis and evaluation of glaucoma.

Optical coherence tomography (OCT) is a commonly used non-invasive imaging modality in glaucoma care that provides structural information about the retina and optic nerve head (ONH). Optical coherence tomography angiography (OCTA) is an extension of OCT that identifies blood flow and vessels, providing non-invasive visualization of retinal microvasculature.[3] In addition to qualitative images, OCTA can also provide quantitative information that can measure and track changes in vasculature as glaucoma progresses. Many studies have quantified OCTA scans using vessel density (VD), a parameter that measures the proportion of the scan occupied by vasculature.[3–6] VD is automatically computed and reported to clinicians in commercially available OCTA devices. Patients with primary open-angle glaucoma (POAG) have reduced VD in the macula and ONH when compared to normal subjects with greater reductions in more advanced stages of disease.[7–11] Additionally, treatment of glaucoma with surgery or IOP-reducing medications has been shown to be associated with recovery of VD, indicating that OCTA may be of use in the longitudinal assessment of glaucoma.[12–14]

Further quantification of vascular quantity and morphology beyond

* Corresponding author. University of Texas at Southwestern Medical Center5323 Harry Hines Boulevard, Dallas, TX. 75390, USA.
E-mail address: Sanjeeva.Kalva2@UTSouthwestern.edu (P. Kalva).

https://doi.org/10.1016/j.aopr.2023.05.002
Received 11 December 2022; Received in revised form 7 May 2023; Accepted 12 May 2023
Available online 12 May 2023

VD may provide additional clinical value in glaucoma care and reveal insights into the pathologic progression of the disease. Quantitative OCTA parameters that convey information about the length and branching of vessels have been well-studied in diabetic retinopathy and found to be of diagnostic value in differentiating healthy and diseased eyes.[15–17] However, their applications are comparatively less explored in glaucoma. The few reported studies in glaucoma are limited by the lack of healthy control groups and small sample sizes with racially homogenous subjects.[18–20]

Therefore, in this study, we evaluated different quantitative measures of the microvasculature in healthy eyes and eyes with POAG imaged with OCTA. In addition, we assessed the diagnostic value of these measures in distinguishing healthy eyes from eyes with glaucoma. We hypothesized that eyes with POAG have both significantly reduced vascular quantity as well as altered morphology that may be of diagnostic value.

2. Methods

2.1. Study population

This retrospective cross-sectional study was approved by the Institutional Review Board (IRB) of the University of Texas at Southwestern Medical Center (UTSW) and adhered to the tenets of the Declaration of Helsinki and the Health Insurance Portability and Accountability Act (HIPAA) of 1996. Due to the retrospective design and lack of direct patient interaction, the IRB did not require patient consent. A total of 98 subjects seen at UTSW's tertiary care glaucoma clinic between January 2020 and May 2020 were included. All subjects had undergone a complete ophthalmologic examination including visual acuity measurement, visual field examination, gonioscopy, dilated fundus photography, tonometry, and OCTA imaging. Inclusion criteria included age >18 years, spherical equivalent $\leq \pm$ 3 diopters, and open angles on gonioscopy. Exclusion criteria included poor scan quality (<6/10 as recommend by the manufacturer), significant scan artifacts, history of ocular trauma, and evidence of vitreoretinal disease, uveitis, hypertensive retinopathy, diabetic retinopathy, Alzheimer's disease, Parkinson's disease, or stroke.

From each included subject, one eye was chosen randomly. Eyes were categorized into healthy and POAG groups. Eyes were classified as healthy if they had normal optic discs, no visual field defects, and IOP <21 mm Hg. Eyes were classified as POAG if they had characteristic optic disc changes (disc cupping, hemorrhages, narrow neuroretinal rim) with corresponding glaucomatous visual field defects with or without elevated IOP. Eyes with POAG were further categorized as mild, moderate, or severe stage based on the Hodapp-Anderson-Parrish criteria using visual field mean deviations.[21]

2.2. Image acquisition

All subjects underwent spectral-domain OCTA imaging with the RTVue XR Avanti (Optovue Inc., Fremont, CA, USA) equipped with AngioVue software version 2018.0.0.18 for visualization of vascular structures. Two scans were captured for each eye with one scan centered around the macula, and the second scan centered around the ONH. The scan area was 3 × 3 mm for macular scans and 4.5 × 4.5 mm for ONH scans. Each ONH scan comprised of 304 B-scans equally spaced on the X-axis and Y-axis with each B-scan consisting of 304 A-scans. Each macular scan comprised of 400 B-scans with each B-scan consisting of 400 A-scans. Eye tracking software was used to reduce the effect of motion-related artifacts.

Built-in software automatically segmented the OCT volume data into predefined layers. We analyzed the superficial and deep layers of the macula and the radial peripapillary capillary (RPC) layer of the ONH. The superficial layer was defined with the inner boundary set at the internal limiting membrane (ILM) and the outer boundary set 10 μm above the inner plexiform layer (IPL). The deep layer was defined at the region from 10 μm above the IPL to 10 μm below the outer plexiform layer (OPL). The RPC layer was defined as the region from the ILM to the posterior boundary of the retinal nerve fiber layer (RNFL) centered around the ONH. Fig. 1 shows healthy and POAG OCTA scans of each layer.

2.3. Image processing and analysis

We measured 3 parameters to quantify vascular morphology: vessel density (VD), vessel length density (VLD), and branchpoint density (BPD). We defined VD as the ratio between the area occupied by vasculature and the total image area. VLD was defined as the ratio

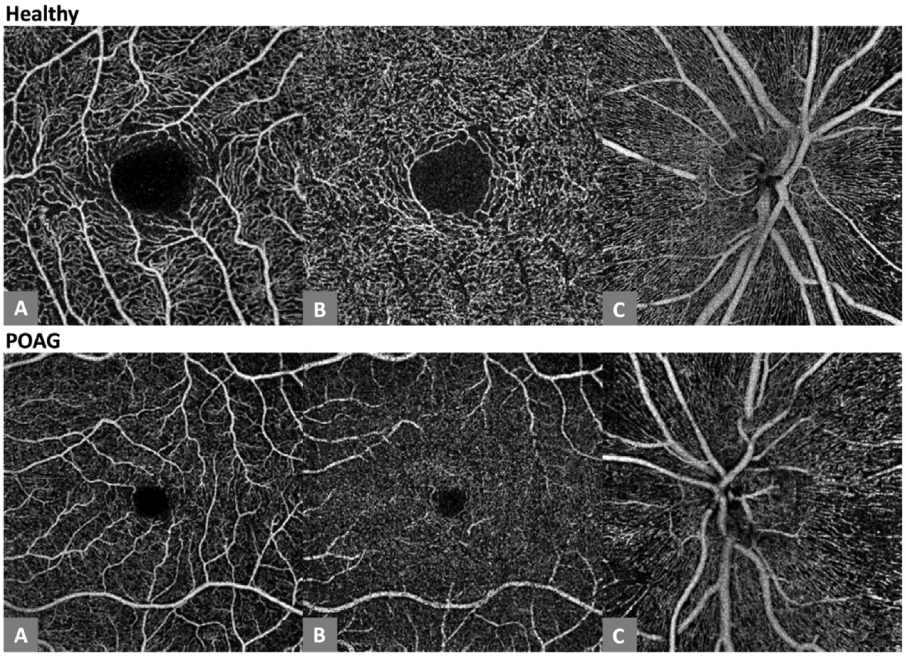

Fig. 1. En face OCTA 3 × 3 OCTA scans of healthy and POAG eyes in the superficial (A), deep (B), and radial peripapillary capillary (RPC) layers (C).

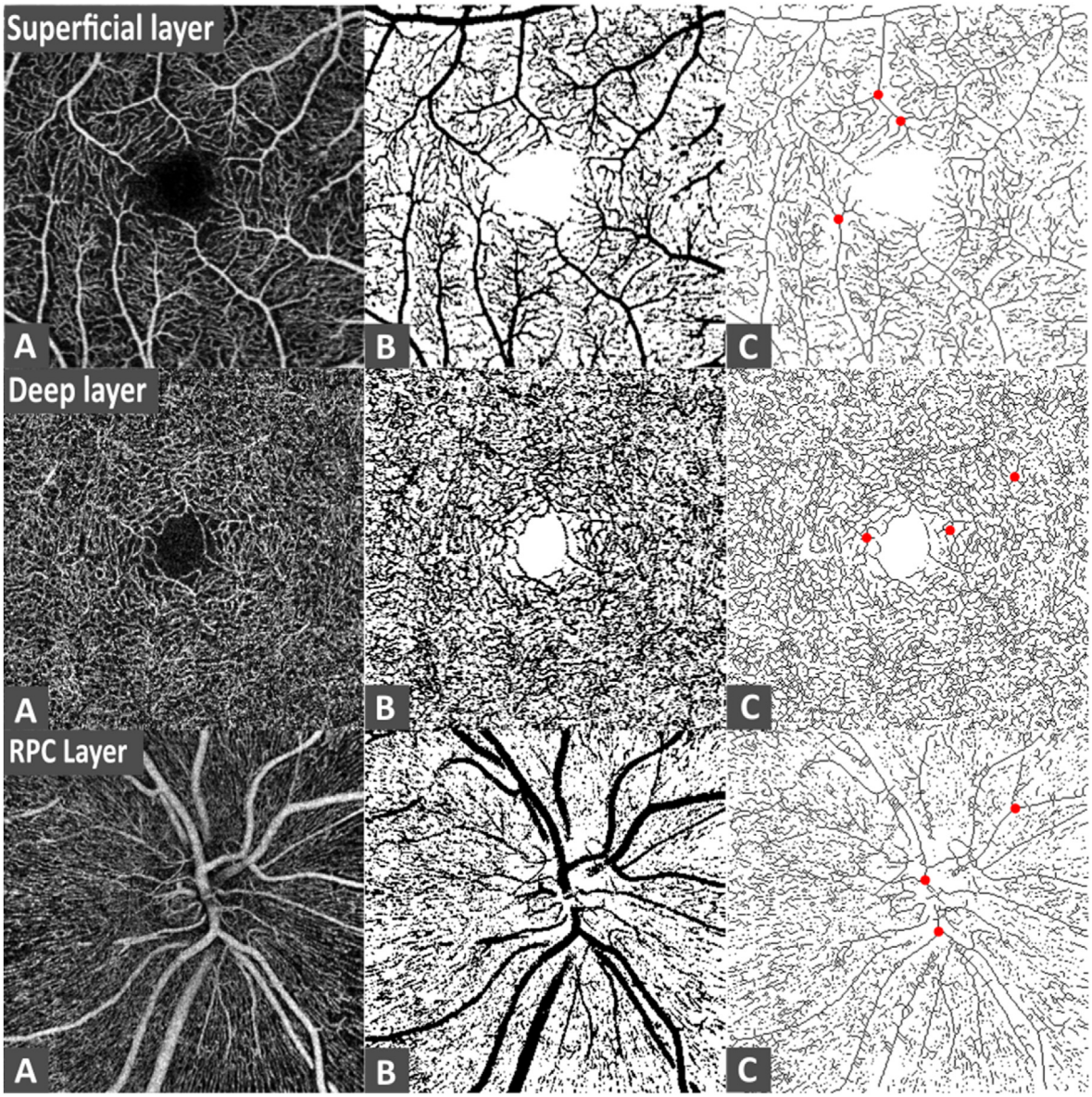

Fig. 2. Image Processing Steps in Vascular Morphology Quantification
A. En face OCTA 3 × 3 mm scan of the superficial layer of a healthy eye. B. Binarized vessel map, used for vessel density calculation. C. Skeletonized vessel map, used for vessel length density and branchpoint density calculations. Red circles show examples of branchpoints.

between the total length of vasculature and the total image area. BPD was defined as the ratio between the total number of vessel branchpoints and the total length of vasculature. Branchpoints were defined as points where vessels divided into two or more vessel branches. All parameters were unitless measures.

All image processing and analysis was performed using ImageJ (National Institute of Health, Bethesda, MD, USA, 2022 version 1.53o). As shown in Fig. 2, a global thresholding algorithm was applied to en face OCTA images to generate binary vessel maps in which each pixel was assigned a value of either 1 (vessel) or 0 (background). We used binary vessel maps to calculate VD. Next, binary vessel maps were used to generate skeletonized vessel maps in which vessel areas were reduced to 1-pixel widths in order to represent the total length of the vascular network. We used the skeletonized vessel maps to calculate VLD and BPD. As shown in red in Fig. 2C, branchpoints were identified from the skeletonized vessel maps as pixels with 3 or more adjacent vessel-containing pixels.

2.4. Statistical analysis

Demographic characteristics and OCTA parameters were compared between the healthy and POAG groups. Continuous variables (age, IOP, RNFL thickness, blood pressure, signal strength index) were compared using Welch's *t*-tests, and categorical variables (sex, race, hypertension, diabetes, and cardiovascular disease) were compared using χ^2 tests. OCTA parameters were compared between groups using linear regression to adjust for any covariates found to be significant in univariate analysis. To determine the diagnostic value of OCTA parameters in differentiating normal and glaucomatous eyes, we performed logistic regression analysis and constructed receiver operating characteristic (ROC) curves for each of the 3 OCTA-derived vascular morphologic parameters in all 3 scan layers. All ROCs were adjusted for covariates found to be significant in univariate analysis. The areas under the curve (AUC) were calculated for each ROC and were compared with the single highest AUC using the De Long test for comparing AUCs.[22] For each regression model, collinearity

Table 1
Characteristics of study participants.

	Healthy	Glaucoma	*P* value
Subjects, *n* (%)	49 (50%)	49 (50%)	
Age, years ± SD	62.8 ± 11.8	71.8 ± 8.2	<0.001
Sex, *n* (%)			0.41
Male	18 (36.7%)	23 (46.9%)	
Female	31 (63.3%)	26 (53.1%)	
Race, *n* (%)			0.78
White	22 (44.9%)	19 (38.8%)	
Black	19 (38.8%)	21 (42.9%)	
Asian	6 (12.2%)	5 (10.2%)	
Other	2 (4.1%)	3 (6.1%)	
Hypertension, *n* (%)	21 (42.9%)	39 (79.6%)	0.48
Diabetes, *n* (%)	16 (32.7%)	16 (32.7%)	1
CV disease, *n* (%)	21 (42.9%)	25 (51.0%)	0.42
Systolic blood pressure, mm Hg ± SD	125.3 ± 14.4	131.1 ± 21.0	0.08
Diastolic blood pressure, mm Hg ± SD	75.5 ± 11.7	77.1 ± 10.0	0.42
IOP, mm Hg ± SD	13.8 ± 3.0	15.0 ± 5.0	0.15
RNFL thickness, μm ± SD	101.1 ± 10.4	74.8 ± 13.8	<0.001
Deep and superficial layer SSI, mean ± SD	67.6 ± 8.7	65.7 ± 7.1	0.18
RPC layer SSI, mean ± SD	62.2 ± 9.0	60.3 ± 7.2	0.25

SD: standard deviation; CV: cardiovascular; IOP: intraocular pressure; RNFL: retinal nerve fiber layer; SSI: signal strength index; RPC: radial peripapillary capillary.

was assessed using variance inflation factor (VIF) tests. All statistical analysis was performed with R version 4.1.2 (R Foundation for Statistical Computing, Vienna, Austria). *P* values < 0.05 were considered statistically significant.

3. Results

A total of 49 eyes from healthy subjects and 49 eyes from subjects with POAG were included in our study. Of the 49 eyes with POAG, 21 eyes had severe POAG, 16 had moderate POAG, and 12 had mild POAG. A summary of the characteristics of study participants is presented in Table 1. Participants with POAG were significantly older (71.8 ± 8.2 years) than healthy participants (62.8 ± 11.8 years) ($P < 0.001$). The mean RNFL thickness in eyes with POAG (74.8 ± 13.8 μm) was lower than in healthy eyes (101.1 ± 10.4 μm) ($P < 0.001$). No statistically significant differences were present between the two groups with respect to sex, race, hypertension, diabetes, cardiovascular disease, systolic blood pressure, diastolic blood pressure, spherical equivalent, IOP, and SSI.

A summary of descriptive statistics for each OCTA parameter measured in the superficial, deep, and RPC layers is presented in Table 2. In all 3 scan layers, VD, VLD, and BPD were significantly reduced in the POAG group compared to the healthy group ($P < 0.001$). There was no overlap in the 95% confidence intervals for all parameters between healthy eyes and eyes with POAG. In both the healthy and POAG groups, the deep layer had the highest mean VD, VLD, and BPD values, followed by the RPC layer, and then the superficial layer. All 3 parameters in the deep layer were found to be significantly different when comparing mild v. moderate POAG, moderate v. severe POAG, and mild v. severe POAG. The parameters in the superficial layer were not significantly different when comparing healthy v. mild POAG, mild v. moderate POAG, and moderate v. severe POAG. For all parameters, the standard deviation was consistently higher in the POAG groups. Since patients with POAG were significantly older than healthy patients ($P < 0.001$), groups were compared using linear regression controlling for age as a covariate.

ROC curves for VD, VLD, and BPD across the 3 scan layers were constructed with adjustment for age and the AUCs for each parameter are presented in Table 3. The overall best performing parameter was the RPC VD [AUC: 0.948 (0.903, 0.992)]. The RPC VD AUC was significantly higher than any parameter's AUC in the superficial or deep layers. No significant differences were found between the RPC VD AUC and the other parameters in the RPC layer. The VIF for each regression model demonstrated low collinearity.

4. Discussion

In this study, we used VD, VLD, and BPD to quantitatively characterize vascular morphology in OCTA scans of the macula and optic disc in healthy and POAG subjects. All parameters were significantly reduced in the eyes of patients with POAG ($P < 0.001$). When comparing parameters across mild, moderate, and severe POAG subjects, all parameters in the deep layer were significantly reduced as severity increased. We also demonstrated the diagnostic value of these parameters in differentiating between normal and glaucomatous eyes. The results of this study complement the known importance of vascular health in glaucoma, as well as highlighting the potential role of vascular morphology in the diagnosis and evaluation of glaucoma.

We found VD to be lower in glaucomatous eyes in both the macula and ONH as reported by many previous studies.[8–10,23] VD reflects the area occupied by vasculature and is theorized to reflect the healthiness of the retinal vascular supply.[3] Higher VD may indicate that the retinal ganglion cells are well-perfused and more resistant to focal or global damage to the vascular network. Most previous studies report average VDs of 0.40–0.50 in healthy eyes, which is higher than the average VDs of 0.25–0.35 seen in our study.[8–10,23,24] This variation is likely caused by differences in VD calculation methods. While previous studies[8–10,23,24] used built-in OCTA software to determine VD, we applied a custom global thresholding algorithm on scans using ImageJ. This was done because we computed the additional parameters of VLD and BPD from the same scan images and thus, it was crucial to use consistent image processing methods for all parameters. Additionally, significant variation has been reported in VD measurements between OCTA devices from different manufacturers, potentially making our results more generalizable than those reported in other studies.[25] Nevertheless, the lower VD in eyes with POAG seen in our study is consistent with findings from other studies.[8–10,23] Individuals with hypertension are known to have lower VD in the deep and superficial layers.[26] In our study, there was no significant differences in blood pressure between the healthy and POAG groups, allowing us to control for this potentially confounding factor.

While VD measures the area occupied by vasculature, VLD reflects the length of the vascular network which is computed by reducing the width of vessels down to 1 pixel. As a result, VLD is theorized to be more sensitive to changes in capillaries and small vessels than VD, potentially being an earlier marker of vascular damage.[17,20,27] As seen in other studies,[17,20,27] we found that VLD was significantly reduced in glaucomatous eyes, suggesting that POAG is associated with reduced vascular network length and capillary perfusion. Future studies investigating VLD

Table 2
Comparison of vascular morphology parameters between healthy and glaucoma groups.

	Healthy (n = 49)	Mild POAG	Moderate POAG	Severe POAG	All POAG	*P* value Healthy v. Mild POAG	*P* value Healthy v. Moderate POAG	*P* value Healthy v. Severe POAG	*P* value Healthy v. All POAG	*P* value Mild v. Moderate POAG	*P* value Mild v. Severe POAG	*P* value Moderate v. Severe POAG
Superficial layer												
VD	0.259 ± 0.028	0.240 ± 0.028	0.199 ± 0.023	0.176 ± 0.029	0.202 ± 0.038	0.072	<0.001	<0.001	<0.001	0.098	0.005	0.081
	(0.250, 0.267)	(0.224, 0.255)	(0.187, 0.211)	(0.163, 0.189)	(0.191, 0.213)							
VLD	0.112 ± 0.015	0.104 ± 0.011	0.085 ± 0.013	0.073 ± 0.012	0.086 ± 0.018	0.164	<0.001	<0.001	<0.001	0.080	<0.001	0.037
	(0.107, 0.116)	(0.098, 0.049)	(0.078, 0.092)	(0.067, 0.078)	(0.080, 0.091)							
BPD	0.049 ± 0.007	0.046 ± 0.006	0.040 ± 0.005	0.037 ± 0.007	0.041 ± 0.007	0.203	<0.001	<0.001	<0.001	0.137	0.021	0.225
	(0.047, 0.051)	(0.042, 0.049)	(0.037, 0.043)	(0.034, 0.040)	(0.038, 0.043)							
Deep layer												
VD	0.343 ± 0.035	0.310 ± 0.042	0.279 ± 0.058	0.237 ± 0.074	0.271 ± 0.068	0.010	<0.001	<0.001	<0.001	0.003	<0.001	0.019
	(0.335, 0.355)	(0.287, 0.333)	(0.249, 0.308)	(0.203, 0.270)	(0.252, 0.290)							
VLD	0.170 ± 0.016	0.153 ± 0.017	0.135 ± 0.025	0.112 ± 0.034	0.131 ± 0.032	0.007	<0.001	<0.001	<0.001	0.007	<0.001	0.010
	(0.165, 0.174)	(0.143, 0.162)	(0.122, 0.148)	(0.097, 0.127)	(0.121, 0.140)							
BPD	0.073 ± 0.009	0.066 ± 0.011	0.059 ± 0.015	0.052 ± 0.018	0.058 ± 0.016	0.036	<0.001	<0.001	<0.001	0.011	<0.001	0.012
	(0.071, 0.076)	(0.060, 0.072)	(0.051, 0.066)	(0.044, 0.059)	(0.053, 0.063)							
RPC layer												
VD	0.313 ± 0.033	0.262 ± 0.044	0.234 ± 0.042	0.202 ± 0.029	0.229 ± 0.044	<0.001	<0.001	<0.001	<0.001	0.097	<0.001	0.017
	(0.303, 0.322)	(0.237, 0.286)	(0.212, 0.255)	(0.190, 0.215)	(0.216, 0.241)							
VLD	0.119 ± 0.011	0.101 ± 0.022	0.086 ± 0.016	0.070 ± 0.014	0.084 ± 0.021	<0.001	<0.001	<0.001	<0.001	0.070	<0.001	0.003
	(0.116, 0.122)	(0.088, 0.113)	(0.078, 0.095)	(0.064, 0.076)	(0.077, 0.090)							
BPD	0.052 ± 0.008	0.042 ± 0.009	0.039 ± 0.008	0.034 ± 0.006	0.038 ± 0.008	<0.001	<0.001	<0.001	<0.001	0.251	<0.001	0.004
	(0.051, 0.055)	(0.037, 0.047)	(0.034, 0.043)	(0.032, 0.037)	(0.035, 0.040)							

Values are presented as mean ± standard deviation (95% confidence interval). *P* values were determined by linear regression to adjust for age as a covariate. Bold indicates significance <0.05. VD: vessel density, VLD: vessel length density, BPD: branchpoint density, RPC: radial peripapillary capillary.

Table 3
Areas under the curve (AUC) for classification of healthy vs glaucomatous eyes.

Scan Layer	Parameter	AUC (95% CI)	VIF	*P* value
Superficial	VD	0.893 (0.832, 0.953)	1.873	0.015
	VLD	0.874 (0.808, 0.940)	1.420	0.026
	BPD	0.833 (0.755, 0.911)	1.033	<0.001
Deep	VD	0.855 (0.784, 0.927)	1.323	0.018
	VLD	0.879 (0.814, 0.943)	1.044	0.026
	BPD	0.832 (0.754, 0.910)	1.105	0.006
RPC	VD	0.948 (0.903, 0.992)	1.390	–
	VLD	0.939 (0.890, 0.988)	1.754	0.523
	BPD	0.934 (0.887, 0.980)	1.062	0.286

AUC: area under the curve; 95% CI: 95% confidence interval, VD: vessel density, VLD: vessel length density, BPD: branchpoint density, RPC: radial peripapillary capillary; VIF.
P values were determined by the DeLong test comparing each parameter with the highest AUC (RPC VD).

should focus specifically on preperimetric and early stage POAG to analyze its theorized value as an early marker of vascular damage.

BPD which measures the level of branching and interconnectedness within the network was also reduced in POAG. This could be because eyes with higher BPD are more resistant to focal occlusions or blockages, and thus, better able to maintain blood supply to the retinal ganglion cells during high vascular stress.[17,27] Additionally, healthier networks with more extensively linked vessels could have higher perfusion capacities. Some studies have examined fractal dimension and vessel tortuosity as parameters to characterize vascular changes in glaucoma, finding significant differences between healthy and diseased eyes.[19,20] While fractal dimension and vessel tortuosity consider the shape and orientation of vessels, BPD focuses specifically on vessel branching and therefore, may offer a different measurement of vascular morphologic changes. To the best of our knowledge, this is the one of the first studies to consider the use of BPD as a parameter in evaluating OCTA scans of eyes with POAG.

In our ROC analysis, we found that all parameters were of good or excellent diagnostic value in differentiating healthy eyes from eyes with POAG. RPC VD, RPC VLD, RPC BPD were the best performing parameters and all 3 has statistically similar AUCs. The excellent performance of all 3 parameters in the RPC layer suggests that analyzing the RPC layer is more useful in detecting POAG than other layers, and that glaucomatous damage is more profound in the RNFL around the ONH. Although parameters in the other scan layers had good performance, the higher discriminatory ability of the RPC layer suggests that it is more associated with early glaucomatous changes. Thinning of the RNFL is well-known to be a sign of glaucoma, and thus, concurrent vascular damage in the area is unsurprising.[28] Previous studies that focused exclusively on VD have also found greater diagnostic value in the ONH region than in the macular region.[3,29] In this study, we have shown that in addition to VD, VLD and BPD have useful discriminatory ability with similar performance in differentiating healthy eyes and eyes with POAG. This may suggest that glaucomatous damage in the RPC layer is associated with damage to capillaries as reflected by the reduced VLD and with a reduction in vessel branching as reflected by the reduced BPD. Structural changes in the optic disc such as cupping are strongly associated with glaucoma and our results suggest that vascular changes in the region may also be indicative of glaucomatous damage. In all 3 layers, BPD had lower diagnostic performance than VD and VLD. One possible explanation for this is that while increased branching may help reduce the effects of focal occlusions, the overall health of retinal ganglion cells is more dependent on global perfusion capacity in these layers.

Our study had several limitations that require consideration. Due to the cross-sectional design of this study, we are unable to make causation claims regarding vascular changes and POAG. In addition, we had a relatively small sample size within each POAG severity group which may have reduced the statistical power of our comparisons. While our study demonstrated the potential diagnostic value of OCTA parameters beyond VD, we did not compare these parameters with traditional OCT parameters such as RNFL thickness. Evaluating OCTA and OCT parameters together may have yielded more accurate classification performance. Furthermore, while 3 × 3 mm scans of the macula were used in this study and several others, 6 × 6 mm scans have been reported to have better diagnostic accuracy in differentiating healthy eyes and eyes with mild POAG.[18,19,29,30] Finally, we excluded scans of poor quality and significant artifacts in this study and thus, the impact of image quality on scan parameters is unclear. Future studies should investigate the effects of image quality as scans obtained in the clinic are often of subpar quality.

5. Conclusions

In conclusion, we investigated 3 quantitative OCTA parameters that characterized the vascular morphology of healthy eyes and eyes with POAG. We found that VD, VLD, and BPD were reduced in glaucomatous eyes, particularly around the ONH. When differentiating between healthy and diseased eyes, RPC VD had the best performance. Our results suggest that quantitative measurements of vascular morphology beyond device-computed VD may provide additional value in the diagnosis and evaluation of glaucoma.

Study approval

The authors confirm that any aspect of the work covered in this manuscript that involved human patients or animals was conducted with the ethical approval of all relevant bodies and the study was performed in accordance with the Declaration of Helsinki.

Author contributions

The authors confirm contribution to the paper as follows: Conception and design of study: PK, KK; Data collection: PK, RA, PM, MS; Analysis and interpretation of results: PK, RA, SS; Drafting the manuscript: PK, RA, KK; All authors reviewed the results and approved the final version of the manuscript.

Funding

This study was supported in part by the NIH grant P30 EY030413 (Bethesda, MD, USA), University of Texas Southwestern Medical Student Research Program (Dallas, TX, USA), and NIH award UL1TR001105.

Declaration of competing interests

The authors declare that they have no known competing financial interests or personal relationships that could have appeared to influence the work reported in this paper.

Acknowledgements

Thanks to all the peer reviewers for their opinions and suggestions.

Abbreviations

OCTA	Optical coherence tomography angiography
VD	Vessel density
VLD	Vessel length density
BPD	Branchpoint density
RPC	Radial peripapillary capillary
ONH	Optic nerve head
AUC	Area under the curve

References

1. Weinreb RN, Aung T, Medeiros FA. The pathophysiology and treatment of glaucoma: a review. *JAMA*. May 14 2014;311(18):1901–1911. https://doi.org/10.1001/jama.2014.3192.
2. Chan KKW, Tang F, Tham CCY, et al. Retinal vasculature in glaucoma: a review. *BMJ Open Ophthalmol*. 2017;1(1), e000032. https://doi.org/10.1136/bmjophth-2016-000032.
3. Rao HL, Pradhan ZS, Suh MH, et al. Optical coherence tomography angiography in glaucoma. *J glaucoma. Apr*. 2020;29(4):312–321. https://doi.org/10.1097/ijg.0000000000001463.
4. Invernizzi A, Cozzi M, Staurenghi G. Optical coherence tomography and optical coherence tomography angiography in uveitis: a review. *Clin Exp Ophthalmol. Apr*. 2019;47(3):357–371. https://doi.org/10.1111/ceo.13470.
5. Sun Z, Yang D, Tang Z, et al. Optical coherence tomography angiography in diabetic retinopathy: an updated review. *Eye (Lond) Jan*. 2021;35(1):149–161. https://doi.org/10.1038/s41433-020-01233-y.
6. Werner AC, Shen LQ. A review of OCT angiography in glaucoma. *Semin Ophthalmol*. 2019;34(4):279–286. https://doi.org/10.1080/08820538.2019.1620807.
7. Liu L, Jia Y, Takusagawa HL, et al. Optical coherence tomography angiography of the peripapillary retina in glaucoma. *JAMA Ophthalmol*. 2015;133(9):1045–1052. https://doi.org/10.1001/jamaophthalmol.2015.2225.
8. Yarmohammadi A, Zangwill LM, Diniz-Filho A, et al. Optical coherence tomography angiography vessel density in healthy, glaucoma suspect, and glaucoma eyes. *Investig Ophthalmol Vis Sci*. 2016;57(9):OCT451–OCT459. https://doi.org/10.1167/iovs.15-18944.
9. El-Nimri NW, Manalastas PIC, Zangwill LM, et al. Superficial and deep macula vessel density in healthy, glaucoma suspect, and glaucoma eyes. *J Glaucoma*. Jun 1 2021;30(6):e276–e284. https://doi.org/10.1097/ijg.0000000000001860.
10. Huo Y, Thomas R, Guo Y, et al. Superficial macular vessel density in eyes with mild, moderate, and severe primary open-angle glaucoma. *Graefe's Arch Clin Exp Ophthalmol*. 2021/07/01 2021;259(7):1955–1963. https://doi.org/10.1007/s00417-021-05120-4.
11. Kumar RS, Anegondi N, Chandapura RS, et al. Discriminant function of optical coherence tomography angiography to determine disease severity in glaucoma. *Invest Ophthalmol Vis Sci Nov 1*. 2016;57(14):6079–6088. https://doi.org/10.1167/iovs.16-19984.
12. Park H-YL, Hong KE, Shin DY, et al. Microvasculature recovery detected using optical coherence tomography angiography and the rate of visual field progression after glaucoma surgery. *Investig Ophthalmol Vis Sci*. 2021;62(15):17. https://doi.org/10.1167/iovs.62.15.17, 17.
13. Liu C, Umapathi RM, Atalay E, et al. The effect of medical lowering of intraocular pressure on peripapillary and macular blood flow as measured by optical coherence tomography angiography in treatment-naive eyes. *J Glaucoma*. Jun 1 2021;30(6):465–472. https://doi.org/10.1097/ijg.0000000000001828.
14. Liu L, Takusagawa HL, Greenwald MF, et al. Optical coherence tomographic angiography study of perfusion recovery after surgical lowering of intraocular pressure. *Sci Rep*. 2021/08/26 2021;11(1), 17251. https://doi.org/10.1038/s41598-021-96225-7.
15. Durbin MK, An L, Shemonski ND, et al. Quantification of retinal microvascular density in optical coherence tomographic angiography images in diabetic retinopathy. *JAMA Ophthalmol*. 2017;135(4):370–376. https://doi.org/10.1001/jamaophthalmol.2017.0080.
16. Alam M, Le D, Lim JI, et al. Vascular complexity analysis in optical coherence tomography angiography of diabetic retinopathy. *Retina Mar 1*. 2021;41(3):538–545. https://doi.org/10.1097/iae.0000000000002874.
17. Chu Z, Lin J, Gao C, et al. Quantitative assessment of the retinal microvasculature using optical coherence tomography angiography. *J Biomed Opt*. 2016;21(6):66008. https://doi.org/10.1117/1.JBO.21.6.066008, 66008.
18. Lin TPH, Wang YM, Ho K, et al. Global assessment of arteriolar, venular and capillary changes in normal tension glaucoma. *Sci Rep*. 2020;10(1):19222. https://doi.org/10.1038/s41598-020-75784-1, 19222.
19. Cheng KKW, Tan BL, Brown L, et al. Macular vessel density, branching complexity and foveal avascular zone size in normal tension glaucoma. *Sci Rep*. 2021;11(1):1056. https://doi.org/10.1038/s41598-020-80080-z, 1056.
20. Richter GM, Sylvester B, Chu Z, et al. Peripapillary microvasculature in the retinal nerve fiber layer in glaucoma by optical coherence tomography angiography: focal structural and functional correlations and diagnostic performance. *Clin Ophthalmol*. 2018;12:2285–2296. https://doi.org/10.2147/opth.S179816.
21. Hodapp E, Parrish RK, Anderson DR. *Clinical Decisions in Glaucoma*. Mosby Incorporated; 1993.
22. DeLong ER, DeLong DM, Clarke-Pearson DL. Comparing the areas under two or more correlated receiver operating characteristic curves: a nonparametric approach. *Biometrics*. 1988;44(3):837–845. https://doi.org/10.2307/2531595.
23. Lu P, Xiao H, Liang C, et al. Quantitative analysis of microvasculature in macular and peripapillary regions in early primary open-angle glaucoma. *Curr Eye Res May*. 2020;45(5):629–635. https://doi.org/10.1080/02713683.2019.1676912.
24. Hong KL, Burkemper B, Urrea AL, et al. Hemiretinal asymmetry in peripapillary vessel density in healthy, glaucoma suspect, and glaucoma eyes. *Am J Ophthalmol*. 2021/10/01/2021;230:156–165. https://doi.org/10.1016/j.ajo.2021.05.019.
25. Arya M, Rebhun CB, Alibhai AY, et al. Parafoveal retinal vessel density assessment by optical coherence tomography angiography in healthy eyes. *Ophthalmic Surg Lasers Imaging Retina*. Oct 15 2018;49(10):S5–s17. https://doi.org/10.3928/23258160-20180814-02.
26. Chua J, Chin CWL, Hong J, et al. Impact of hypertension on retinal capillary microvasculature using optical coherence tomographic angiography. *J Hypertens Mar*. 2019;37(3):572–580. https://doi.org/10.1097/hjh.0000000000001916.
27. Corliss BA, Mathews C, Doty R, et al. Methods to label, image, and analyze the complex structural architectures of microvascular networks. *Microcirculation*. 2019;26(5), e12520-e12520. https://doi.org/10.1111/micc.12520.
28. Bowd C, Zangwill LM, Berry CC, et al. Detecting early glaucoma by assessment of retinal nerve fiber layer thickness and visual function. *Investig Ophthalmol Vis Sci*. 2001;42(9):1993–2003.
29. Hou T-Y, Kuang T-M, Ko Y-C, et al. Optic disc and macular vessel density measured by optical coherence tomography angiography in open-angle and angle-closure glaucoma. *Sci Rep*. 2020/03/27 2020;10(1):5608. https://doi.org/10.1038/s41598-020-62633-4.
30. Penteado RC, Bowd C, Proudfoot JA, et al. Diagnostic ability of optical coherence tomography angiography macula vessel density for the diagnosis of glaucoma using difference scan sizes. *J Glaucoma*. 2020;29(4):245–251. https://doi.org/10.1097/ijg.0000000000001447.